

<https://doi.org/10.3799/dqkx.2019.234>



蚀变洋壳和俯冲带变质流体的 Fe-Mg 同位素组成

黄建, 黄方, 肖益林

中国科学院壳幔物质与环境重点实验室, 中国科学技术大学地球和空间科学学院, 安徽合肥 230026

摘要: 贫碳酸盐的蚀变洋壳具有与新鲜洋中脊玄武岩一致的 Mg 同位素组成, 说明低温和高温洋壳蚀变不会导致 Mg 同位素分馏. 大别山港河和花凉亭的早期变质脉比榴辉岩具有偏高的 $\delta^{56}\text{Fe}$ - $\delta^{26}\text{Mg}$ 值, 而且早期到晚期变质脉的 $\delta^{56}\text{Fe}$ - $\delta^{26}\text{Mg}$ 值逐渐降低. 这些结果说明, 在流体-岩石反应和流体演化过程中, Fe-Mg 同位素发生了显著的分馏, 且矿物溶解-再沉淀是同位素分馏的控制因素. 相比洋中脊玄武岩, 蚀变洋壳和变质脉具有相似或偏高的 $\delta^{56}\text{Fe}$ - $\delta^{26}\text{Mg}$ 值, 说明蚀变洋壳脱水产生的流体富集重 Fe-Mg 同位素, 不能解释弧岩浆岩的轻 Fe/重 Mg 同位素组成. 因此, 弧岩浆岩异常的 Fe-Mg 同位素组成是熔体提取和富集 ^{54}Fe - ^{26}Mg 的蛇纹岩流体交代地幔楔两个过程共同作用的结果.

关键词: 铁-镁同位素; 蚀变洋壳; 榴辉岩; 变质流体; 流体演化; 弧岩浆岩; 地球化学.

中图分类号: P581

文章编号: 1000-2383(2019)12-4050-07

收稿日期: 2019-08-16

Fe-Mg Isotopic Compositions of Altered Oceanic Crust and Subduction-Zone Fluids

Huang Jian, Huang Fang, Xiao Yilin

CAS Key Laboratory of Crust-Mantle Materials and Environments, School of Earth and Space Sciences, University of Science and Technology of China, Hefei 230026, China

Abstract: The origin of the light Fe and heavy Mg isotope enrichments in arc lavas remains unclear because of the lack of constraints on the Fe-Mg isotope compositions of altered oceanic crust (AOC) and metamorphic fluids in subduction zones. Carbonate-barren AOC has Mg isotope compositions similar to those of fresh mid-ocean ridge basalts, suggesting that low-to-high temperature alteration of oceanic crust by seawater and hydrothermal fluids results in limited Mg isotope fractionation. Fe-Mg isotope measurements show that the early omphacite-epidote veins have higher $\delta^{56}\text{Fe}$ and $\delta^{26}\text{Mg}$ compared to the host eclogites and that the $\delta^{56}\text{Fe}$ and $\delta^{26}\text{Mg}$ gradually decrease from the early omphacite-epidote through epidote-quartz to the late kyanite-epidote-quartz veins. These results indicate significant Fe-Mg isotope fractionation during fluid-rock interaction and fluid evolution due to the dissolution-precipitation processes of minerals in subduction zones. Compared to mid-ocean ridge basalts, the similar or higher $\delta^{56}\text{Fe}$ and $\delta^{26}\text{Mg}$ of AOC and metamorphic veins suggest that AOC-derived fluids are probably enriched in heavy Fe-Mg isotopes. Thus, contribution from AOC-derived fluids is unlikely to explain the light Fe and heavy Mg isotope compositions of arc lavas. We propose that the Fe-Mg isotope anomaly of arc lavas may result from a combination of prior melt depletion and addition of serpentinite-derived ^{54}Fe - ^{26}Mg -rich fluids into the overlying mantle wedge.

Key words: Fe-Mg isotopes; altered oceanic crust; eclogite; metamorphic fluids; fluid evolution; arc lavas; geochemistry.

基金项目: 国家重点基础研究发展计划项目(No.2015CB856102); 国家自然科学基金项目(No.41573018).

作者简介: 黄建(1984-), 男, 博士, 副研究员, 从事金属稳定同位素和地幔地球化学研究. ORCID: 0000-0001-8651-814X. E-mail: jianhuang@ustc.edu.cn

引用格式: 黄建, 黄方, 肖益林, 2019. 蚀变洋壳和俯冲带变质流体的 Fe-Mg 同位素组成. 地球科学, 44(12):4050-4056.

0 引言

在板块汇聚边缘,俯冲板片脱水或熔融产生流体或熔体,交代上覆地幔楔,引发地幔楔部分熔融,产生弧岩浆岩.板片熔流体是俯冲带壳-幔相互作用的重要媒介,会导致弧岩浆岩相比洋中脊玄武岩富集大离子亲石(如 K、Rb、Sr 和 Ba)和轻稀土(如 La 和 Ce)元素,亏损高场强元素(如 Nb 和 Ta)(Elliott *et al.*, 1997).板片熔流体的主要源区为沉积物、蚀变洋壳和蛇纹岩(Schmidt and Poli, 1998).对板片熔流体来源的认识将有助于阐明壳-幔相互作用的过程以及俯冲带板片物质进入地幔楔的方式.

除了微量元素和放射成因(如 Sr-Nd-Pb)同位素,金属 Fe-Mg 稳定同位素也能制约板片熔流体的性质和来源.相比亏损地幔,原始弧岩浆岩($Mg^{#} \geq 0.60$)具有较高的 $\delta^{26}Mg$ ($-0.35\text{‰} \sim -0.06\text{‰}$; Teng *et al.*, 2016; Li *et al.*, 2017) 和较大的 $\delta^{56}Fe$ 变化范围 ($-0.15\text{‰} \sim -0.14\text{‰}$; Dauphas *et al.*, 2009; Nebel *et al.*, 2013, 2015; Foden *et al.*, 2018).原始弧岩浆岩的轻 Fe/重 Mg 同位素组成被认为是富集 ^{54}Fe - ^{26}Mg 的板片熔流体交代弧下地幔楔所致(Nebel *et al.*, 2015; Sossi *et al.*, 2016; Teng *et al.*, 2016).Fe-Mg-Sr-Nd-Pb-Hf 同位素联合模拟显示,沉积物来源的熔流体不能解释原始弧岩浆岩富集轻

Fe/重 Mg 同位素的特征(Nebel *et al.*, 2015; Teng *et al.*, 2016; Foden *et al.*, 2018).因此,蚀变洋壳或蛇纹岩可能是富集 ^{54}Fe - ^{26}Mg 板片熔流体的主要来源(Chen *et al.*, 2016; Debret *et al.*, 2016; Sossi *et al.*, 2016; Teng *et al.*, 2016).然而,由于不清楚蚀变洋壳和变质流体的 Fe-Mg 同位素组成以及变质流体形成和演化过程中 Fe-Mg 同位素的分馏行为,极大地制约了我们对原始弧岩浆岩 Fe-Mg 同位素异常的理解.针对上述问题,本文综述了东太平洋 IODP 1256 钻孔蚀变洋壳以及大别山超高压榴辉岩和变质脉的 Fe-Mg 同位素的研究.

1 蚀变洋壳

蚀变洋壳样品取自位于东太平洋的 IODP 1256 钻孔.洋壳的年龄约为 15 Ma,是在洋中脊超快速扩张时形成(200 mm/a).IODP 1256 钻孔恢复了迄今为止最为完整的洋壳,包括火山岩、过渡带、席状岩墙和侵入岩等 4 个部分(图 1).低-高温蚀变矿物的出现和高度变化的 $\delta^{18}O$ (图 1a, 1b) 显示,洋壳经历低温海水和高温热液蚀变作用.我们精心挑选的 44 个蚀变洋壳样品涵盖了 4 个不同的部分.Mg 同位素分析结果显示,除了一个样品具有偏高的 $\delta^{26}Mg$,其他样品具有相对均一的 $\delta^{26}Mg$ ($-0.36\text{‰} \sim -0.14\text{‰}$) (图 1c).

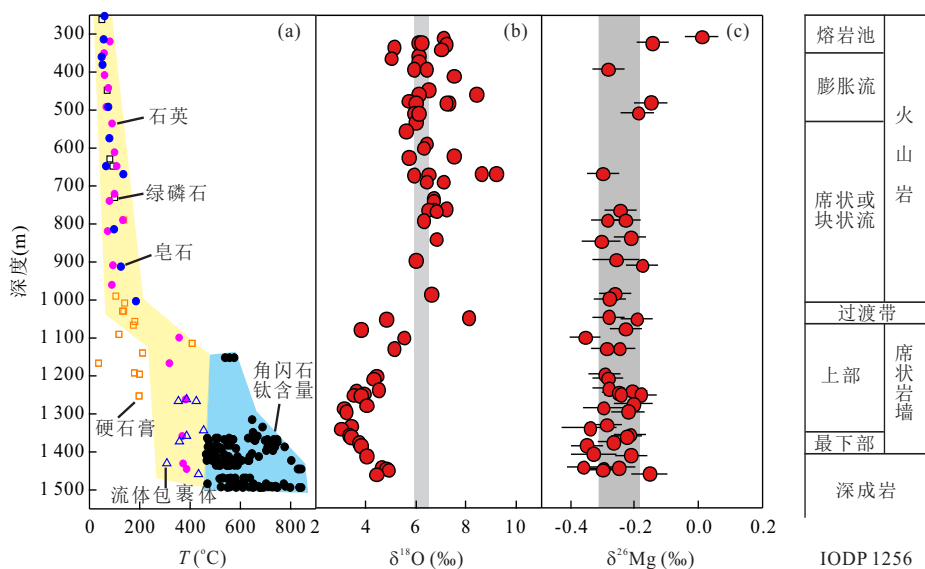


图 1 IODP 1256 钻孔洋壳的蚀变温度(a), $\delta^{18}O$ (b)和 $\delta^{26}Mg$ (c)的空间变化

Fig.1 Down-hole variations in alteration temperatures, $\delta^{18}O$, and $\delta^{26}Mg$ of oceanic crust from IODP site 1256

蚀变温度、O 和 Mg 同位素数据引自 Alt *et al.* (2010)、Gao *et al.* (2012) 和 Huang *et al.* (2015).灰色条带表示新鲜洋中脊玄武岩的 O 和 Mg 同位素组成(Harmon and Hoefs, 1995; Teng *et al.*, 2010)

2 大别山榴辉岩和变质脉

大别山超高压变质带位于大别—苏鲁超高压造山带的西南部(Zheng *et al.*, 2003). 榴辉岩和变质脉采自大别山港河和花凉亭. 根据矿物组合, 变质脉分为绿辉石—绿帘石、绿帘石—石英和蓝晶石—绿帘石—石英脉. 详细的岩相学、矿物学和地球化学特征请见 Guo *et al.* (2012, 2013, 2014, 2015). 两地榴辉岩含有硬柱石脱水后形成的绿帘石+蓝晶石+石英柱状集合体, 且它们的模式丰度向脉体方向逐渐降低; 同时, 在蓝晶石中发现柯石英; 另外, 榴辉岩与变质脉具有相似的 Sr 同位素组成. 最后, 榴辉岩具有系统变化的主微量元素含量. 这些证据说明, 初始流体是硬柱石在超高压变质阶段脱水产

生, 然后与榴辉岩反应, 溶解其中的矿物(如绿帘石、蓝晶石、石英和绿辉石等), 最后形成溶质富集的成脉流体. 绿辉石—绿帘石脉最早从成脉流体中固结形成, 接着形成的是绿帘石—石英脉, 最后形成的是蓝晶石—绿帘石—石英脉.

图 2 和图 3 总结了大别山港河和花凉亭榴辉岩、变质脉和单矿物的 Fe-Mg 同位素分析结果. 如图 2 所示, 相比远离脉的榴辉岩, 靠近脉的榴辉岩具有相似或略微偏轻的 Fe-Mg 同位素组成; 相比榴辉岩, 绿辉石—绿帘石脉富集重 Fe-Mg 同位素; 从早期绿辉石—绿帘石脉到晚期蓝晶石—绿帘石—石英脉, $\delta^{56}\text{Fe}$ 和 $\delta^{26}\text{Mg}$ 值逐渐降低. 如图 3 所示, 相比石榴石, 绿辉石、绿帘石和多硅白云母富集重 Fe-Mg 同位素.

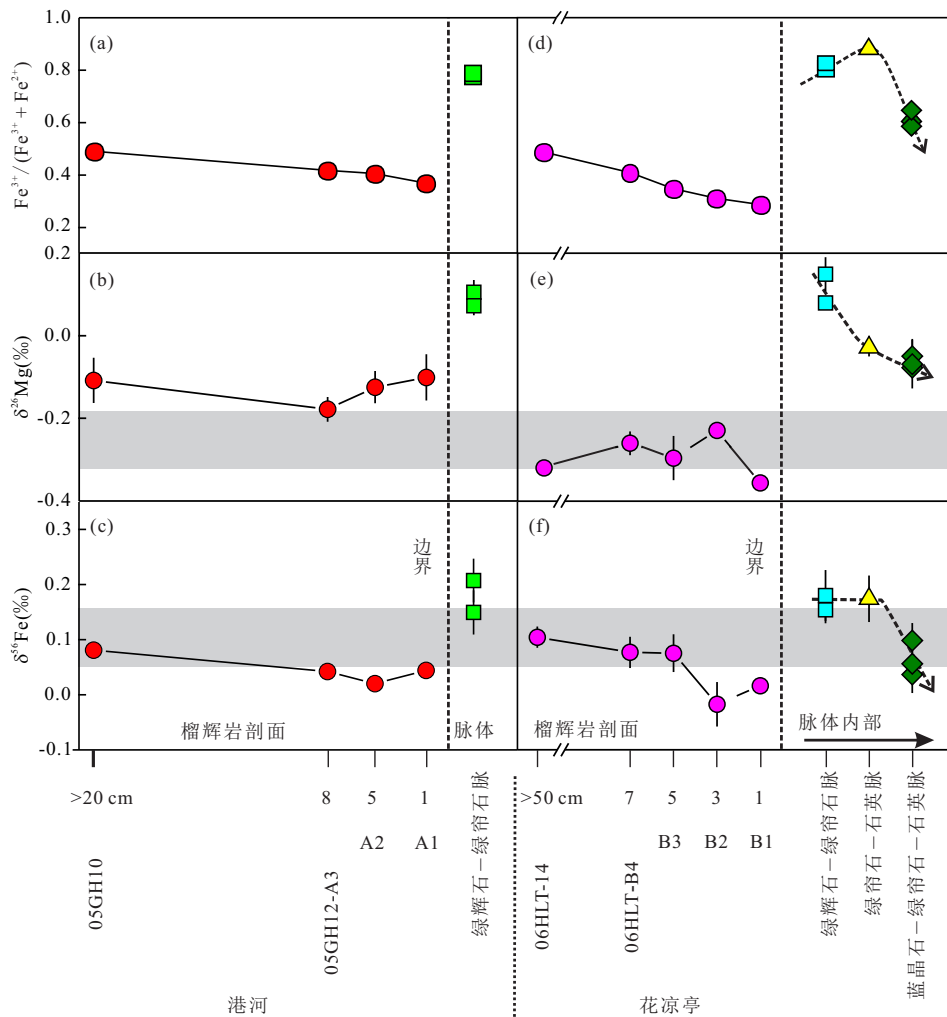


图 2 大别山港河和花凉亭榴辉岩和变质脉的 $\text{Fe}^{3+}/\Sigma\text{Fe}$, $\delta^{26}\text{Mg}$ 和 $\delta^{56}\text{Fe}$ 变化

Fig. 2 $\text{Fe}^{3+}/\Sigma\text{Fe}$, $\delta^{26}\text{Mg}$, and $\delta^{56}\text{Fe}$ in eclogites and veins at Ganghe and Hualiangting in the Dabie orogen

据 Huang *et al.* (2019). 灰色条带表示新鲜洋中脊玄武岩的 Fe-Mg 同位素组成 (Weyer and Ionov, 2007; Teng *et al.*, 2010; Nebel *et al.*, 2013)

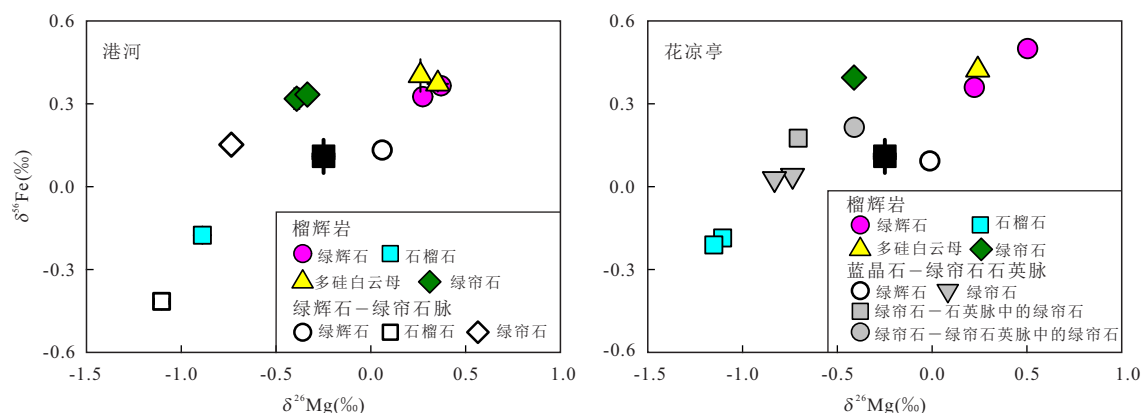


图 3 大别山港河和花凉亭超高压榴辉岩和变质脉中矿物的 Fe-Mg 同位素组成

Fig. 3 $\delta^{26}\text{Mg}$ and $\delta^{56}\text{Fe}$ of minerals from eclogites and veins at Ganghe and Hualiangting in the Dabie orogen

据 Huang *et al.* (2019). 黑色正方形表示新鲜洋中脊玄武岩的 Fe-Mg 同位素组成 (Weyer and Ionov, 2007; Teng *et al.*, 2010; Nebel *et al.*, 2013)

2.1 流体-岩石相互作用过程中的 Fe-Mg 同位素分馏

根据绿片岩到榴辉岩具有相似的 Fe-Mg 同位素组成,前人提出玄武质岩石脱水不会产生 Fe-Mg 同位素分馏 (Wang *et al.*, 2014; El Korh *et al.*, 2017; Inglis *et al.*, 2017). 但是,我们发现绿辉石-绿帘石脉比围岩榴辉岩具有较高的 $\delta^{56}\text{Fe}$ 和 $\delta^{26}\text{Mg}$ (图 2), 说明流体-岩石反应能够导致显著的 Fe-Mg 同位素分馏. 岩石学和地球化学证据证实,榴辉岩中硬柱石在 ~ 3.0 GPa 和 ~ 670 °C 条件下,脱水产生初始流体,初始流体与榴辉岩反应,溶解其中的绿辉石、绿帘石、蓝晶石、石英、金红石、锆石和磷灰石等矿物,迁移大量的元素进入成脉流体中,最终形成绿辉石-绿帘石脉. 与石榴石相比,绿辉石和绿帘石具有较高的 $\text{Fe}^{3+}/\Sigma\text{Fe}$ (Li *et al.*, 2005), 且相对富集重 Fe-Mg 同位素 (图 3). 因此,绿辉石和绿帘石溶解会导致榴辉岩的 $\text{Fe}^{3+}/\Sigma\text{Fe}$ 逐渐降低,同时优先运移 Fe^{3+} 、 ^{56}Fe 和 ^{26}Mg 进入成脉流体中. 绿辉石-绿帘石脉从这种成脉流体中结晶分离出来,从而具有高的 $\text{Fe}^{3+}/\Sigma\text{Fe}$ 、 $\delta^{56}\text{Fe}$ 和 $\delta^{26}\text{Mg}$ 值 (图 2).

2.2 流体演化过程中的 Fe-Mg 同位素分馏

花凉亭多期变质脉记录了俯冲带流体的演化过程. 绿辉石-绿帘石、绿帘石-石英和蓝晶石-绿帘石-石英脉相继从同一成脉流体中结晶沉淀出来 (Guo *et al.*, 2015). 在花凉亭变质脉中,绿帘石的 $\text{Eu}/\text{Eu}^* [\text{Eu}_\text{N}/(\text{Sm}_\text{N}\cdot\text{Gd}_\text{N})^{-0.5}]$ 可以反映成脉流体的演化过程,因为绿帘石是轻稀土元素的主要寄主矿物,且绿帘石与流体之间 Eu 的分配系数大于 Sm 和 Gd (Feineman *et al.*, 2007; Martin *et al.*, 2011). 全岩和绿帘石系统变化的 Eu/Eu^* (图 4) 是矿物连续分离结晶的结果. $\delta^{56}\text{Fe}$ 和 $\delta^{26}\text{Mg}$ 与 Eu/Eu^* 呈正相关

性,说明脉体变化的 Fe-Mg 同位素组成是流体演化过程中,矿物-流体之间 Fe-Mg 同位素平衡分馏的结果. 因为绿辉石和绿帘石相对富集 ^{56}Fe 和 ^{26}Mg (图 3), 它们的分离结晶会降低残余流体的 $\delta^{56}\text{Fe}$ 和 $\delta^{26}\text{Mg}$, 使得后期形成的绿帘石-石英和蓝晶石-绿帘石-石英脉具有较低的 $\delta^{56}\text{Fe}$ 和 $\delta^{26}\text{Mg}$. 综合 2.1 和 2.2 节,我们认为矿物溶解-再沉淀导致了俯冲带变质流体的 Fe-Mg 同位素组成的高度变化.

3 弧岩浆岩 Fe-Mg 同位素异常的成因

相比洋中脊玄武岩 ($\delta^{56}\text{Fe}=0.11\text{‰}\pm 0.06\text{‰}$; Weyer and Ionov, 2007; Nebel *et al.*, 2013; Teng *et al.*, 2013), 弧岩浆岩的 $\delta^{56}\text{Fe}$ 具有较大的变化范围 ($-0.15\text{‰}\sim 0.71\text{‰}$; Dauphas *et al.*, 2009; Nebel *et al.*, 2013, 2015; Foden *et al.*, 2018). 部分熔融会导致玄武质熔体相对地幔源区富集 ^{56}Fe ; 岩浆演化过程中,矿物的分离结晶致使残余熔体进一步富集 ^{56}Fe . 因此,弧岩浆岩的重 Fe 同位素组成可能是部分熔融和岩浆演化共同作用的结果. 但是,大部分原始弧岩浆 ($\text{Mg}^\# \geq 0.60$) 富集轻 Fe/重 Mg 同位素 (Dauphas *et al.*, 2009; Nebel *et al.*, 2013, 2015; Teng *et al.*, 2016; Li *et al.*, 2017; Foden *et al.*, 2018), 不能用部分熔融和岩浆演化来解释. 由于流体优先从沉积物中淋滤出 ^{54}Fe (Inglis *et al.*, 2017; Debret *et al.*, 2018), 沉积物脱水形成的流体具有轻 Fe 同位素组成. 沉积物来源的流体可以具有轻或重 Mg 同位素组成,取决于富集 ^{24}Mg 碳酸盐的溶解,还是富集 ^{26}Mg 白云母和黑云母的溶解 (Wang *et al.*, 2017). 但是, Fe-Mg-Sr-Nd-Pb-Hf 同位素联合模拟显示,沉积物来源的流体不

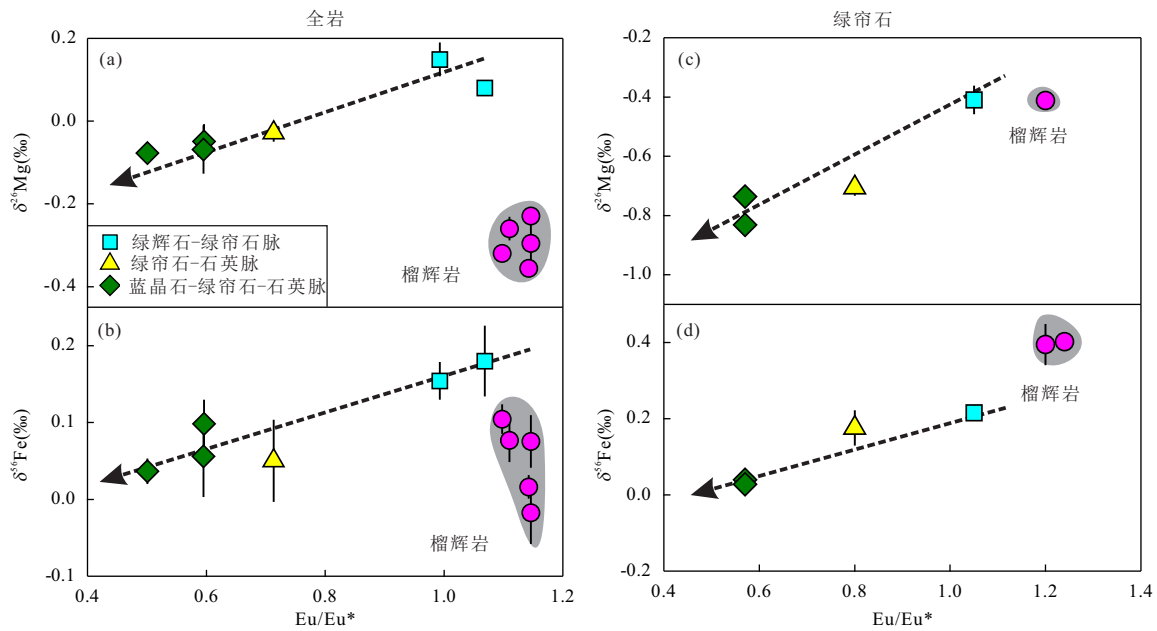


图4 大别山花凉亭三期变质脉全岩(a,b)和绿帘石(c,d)的Eu/Eu*、 $\delta^{26}\text{Mg}$ 和 $\delta^{56}\text{Fe}$ 协变图解

Fig.4 Eu/Eu*, $\delta^{26}\text{Mg}$, and $\delta^{56}\text{Fe}$ in whole-rocks (a, b) and epidotes (c, d) of multi-stage veins at Hualiangting in the Dabie orogen
据 Huang *et al.* (2019)

能解释原始弧岩浆岩 Fe-Mg 同位素异常 (Nebel *et al.*, 2015; Teng *et al.*, 2016; Foden *et al.*, 2018). 因此, 蛇纹岩或蚀变洋壳来源的熔流体成为一种选择 (Sossi *et al.*, 2016; Teng *et al.*, 2016; Li *et al.*, 2017).

大别山港河和花凉亭榴辉岩的原岩是大陆玄武岩, 它们的主量元素含量与蚀变洋壳相似. 因此, 港河和花凉亭榴辉岩脱水可以类比为蚀变洋壳在榴辉岩相变质脱水. 变质脉的 $\delta^{56}\text{Fe}$ (0.04‰~0.21‰) 和 $\delta^{26}\text{Mg}$ (-0.08‰~0.15‰) 高于亏损地幔 ($\delta^{56}\text{Fe}=0.03\text{‰}\pm 0.03\text{‰}$, Craddock *et al.*, 2013; $\delta^{26}\text{Mg}=-0.25\text{‰}\pm 0.07\text{‰}$, Teng *et al.*, 2013), 暗示蚀变洋壳来源的流体具有偏重的 Fe-Mg 同位素组成, 不能解释弧岩浆岩的轻 Fe 和重 Mg 同位素特征. 蚀变洋壳具有与洋中脊玄武岩一致或偏重的 Mg 同位素组成 (图 1) 也支持这一结论.

蛇纹石和滑石是蛇纹岩中重要的富水和富 Mg 矿物. 滑石非常富集 ^{26}Mg , 其脱水会导致蛇纹岩流体具有较高的 $\delta^{26}\text{Mg}$ 值 (0.42‰~0.95‰; Chen *et al.*, 2016). 蛇纹石富集 ^{54}Fe (Scott *et al.*, 2017), 同时蛇纹岩来源的流体一般富集 $\text{Fe}^{2+}\text{SO}_x$ 或 $\text{Fe}^{2+}\text{Cl}_2$ (Debret *et al.*, 2016), 而 $\text{Fe}^{2+}\text{SO}_x$ 或 $\text{Fe}^{2+}\text{Cl}_2$ 相对富集 ^{54}Fe (Dauphas *et al.*, 2017). 因此, 蛇纹岩脱水产生的流体富集 ^{54}Fe (Debret *et al.*, 2016). 在 Kohistan 弧下地幔中, 从富 S-Cl 的蛇纹岩流体中结晶的橄榄石的 $\delta^{56}\text{Fe}$ 低至 -0.36‰ (Debret

et al., 2018). 结合橄榄石与富 S-Cl 流体之间的 Fe 同位素分馏系数 (即 500 °C 时, $\Delta^{56}\text{Fe}_{\text{橄榄石}-\text{Fe}_2+\text{SO}_4(\text{H}_2\text{O})_5} = 0.09\text{‰}$, $\Delta^{56}\text{Fe}_{\text{橄榄石}-\text{Fe}_2+\text{Cl}_2(\text{H}_2\text{O})_5} = 0.22\text{‰}$; Dauphas *et al.*, 2017), 估计得到蛇纹岩流体的 $\delta^{56}\text{Fe}$ 可以低至 -0.58‰~-0.45‰. 同时, 多相固体和高压变质脉研究结果显示, 蛇纹岩来源的流体具有变化较大但总体偏高的 MgO (1.05‰~39.8%) 和 FeO (1.02‰~15.9%) 含量 (Debret *et al.*, 2016). 因此, 弧岩浆岩 Fe-Mg 同位素异常是由富集 ^{54}Fe - ^{26}Mg 的蛇纹岩流体交代弧下地幔楔导致的. 这一解释与地幔楔橄榄岩具有高 $\delta^{26}\text{Mg}$ (-0.26‰~-0.06‰) 和低 $\delta^{56}\text{Fe}$ (-0.38‰~0‰) 的结果相吻合 (Williams *et al.*, 2005; Pogge von Strandmann *et al.*, 2011; Turner *et al.*, 2018).

4 结论

根据贫碳酸盐的蚀变洋壳以及大别山超高压榴辉岩和变质脉的高精度 Fe-Mg 同位素数据, 可以得出以下结论.

(1) 东太平洋 IODP 1256 钻孔贫碳酸盐的蚀变洋壳具有与新鲜洋中脊玄武岩一致的 Mg 同位素组成, 说明低温海水和高温热液蚀变不会导致 Mg 同位素分馏.

(2) 相比围岩榴辉岩, 早期绿辉石-绿帘石脉富集重 Fe-Mg 同位素; 相比绿辉石-绿帘石脉, 晚期绿帘

石—石英和蓝晶石—绿帘石—石英脉的 $\delta^{56}\text{Fe}$ 和 $\delta^{26}\text{Mg}$ 值逐渐降低。这些结果说明, 在流体—岩石反应和流体演化过程中, Fe-Mg 同位素发生了显著的分馏, 且矿物溶解-再沉淀是 Fe-Mg 同位素分馏的控制因素。

(3) 蚀变洋壳来源的流体比亏损地幔具有偏重的 Fe-Mg 同位素组成, 不能解释弧岩浆岩富集轻 Fe/重 Mg 同位素的特征。因此, 弧岩浆岩 Fe-Mg 同位素异常可能是熔体提取和富集 ^{54}Fe - ^{26}Mg 的蛇纹岩流体交代地幔楔两个过程共同作用的结果。

致谢: 感谢郑永飞院士和陈伊翔教授的邀稿, 感谢郭顺博士和高永军博士提供宝贵的样品, 感谢审稿专家提出的建设性意见!

References

- Alt, J.C., Laverne, C., Coggon, R.M., et al., 2010. Subsurface Structure of a Submarine Hydrothermal System in Ocean Crust Formed at the East Pacific Rise, ODP/IODP Site 1256. *Geochemistry, Geophysics, Geosystems*, 11(10): Q10010. <https://doi.org/10.1029/2010gc003144>
- Chen, Y.X., Schertl, H.P., Zheng, Y.F., et al., 2016. Mg-O Isotopes Trace the Origin of Mg-Rich Fluids in the Deeply Subducted Continental Crust of Western Alps. *Earth and Planetary Science Letters*, 456: 157–167. <https://doi.org/10.1016/j.epsl.2016.09.010>
- Craddock, P.R., Warren, J.M., Dauphas, N., 2013. Abyssal Peridotites Reveal the Near-Chondritic Fe Isotopic Composition of the Earth. *Earth and Planetary Science Letters*, 365: 63–76. <https://doi.org/10.1016/j.epsl.2013.01.011>
- Dauphas, N., Craddock, P.R., Asimow, P.D., et al., 2009. Iron Isotopes May Reveal the Redox Conditions of Mantle Melting from Archean to Present. *Earth and Planetary Science Letters*, 288(1–2): 255–267. <https://doi.org/10.1016/j.epsl.2009.09.029>
- Dauphas, N., John, S.G., Rouxel, O., 2017. Iron Isotope Systematics. *Reviews in Mineralogy and Geochemistry*, 82(1): 415–510. <https://doi.org/10.2138/rmg.2017.82.11>
- Debret, B., Bouilhol, P., Pons, L., et al., 2018. Carbonate Transfer during the Onset of Slab Devolatilization: New Insights from Fe and Zn Stable Isotopes. *Journal of Petrology*, 59(6): 1145–1166. <https://doi.org/10.1093/ptrology/egy057v>
- Debret, B., Millet, M.A., Pons, M.L., et al., 2016. Isotopic Evidence for Iron Mobility during Subduction. *Geology*, 44(3): 215–218. <https://doi.org/10.1130/g37565.1>
- El Korh, A., Luais, B., Delouie, E., et al., 2017. Iron Isotope Fractionation in Subduction-Related High-Pressure Metabasites (Ile de Groix, France). *Contributions to Mineralogy and Petrology*, 172: 41. <https://doi.org/10.1007/s00410-017-1357-x>
- Elliott, T., Plank, T., Zindler, A., et al., 1997. Element Transport from Slab to Volcanic Front at the Mariana Arc. *Journal of Geophysical Research: Solid Earth*, 102(B7): 14991–15019.
- Feineman, M.D., Ryerson, F.J., DePaolo, D.J., et al., 2007. Zoisite-Aqueous Fluid Trace Element Partitioning with Implications for Subduction Zone Fluid Composition. *Chemical Geology*, 239(3–4): 250–265. <https://doi.org/10.1016/j.chemgeo.2007.01.008>
- Foden, J., Sossi, P.A., Nebel, O., 2018. Controls on the Iron Isotopic Composition of Global Arc Magmas. *Earth and Planetary Science Letters*, 494: 190–201. <https://doi.org/10.1016/j.epsl.2018.04.039>
- Gao, Y.J., Vils, F., Cooper, K.M., et al., 2012. Downhole Variation of Lithium and Oxygen Isotopic Compositions of Oceanic Crust at East Pacific Rise, ODP Site 1256. *Geochemistry, Geophysics, Geosystems*, 13(10): Q10001. <https://doi.org/10.1029/2012gc004207>
- Guo, S., Chen, Y., Ye, K., et al., 2015. Formation of Multiple High-Pressure Veins in Ultrahigh-Pressure Eclogite (Hualiangting, Dabie Terrane, China): Fluid Source, Element Transfer, and Closed-System Metamorphic Veining. *Chemical Geology*, 417: 238–260. <https://doi.org/10.1016/j.chemgeo.2015.10.006>
- Guo, S., Ye, K., Chen, Y., et al., 2012. Fluid-Rock Interaction and Element Mobilization in UHP Metabasalt: Constraints from an Omphacite-Epidote Vein and Host Eclogites in the Dabie Orogen. *Lithos*, 136–139: 145–167. <https://doi.org/10.1016/j.lithos.2011.11.008>
- Guo, S., Ye, K., Wu, T.F., et al., 2013. A Potential Method to Confirm the Previous Existence of Lawsonite in Eclogite: The Mass Imbalance of Sr and LREEs in Multistage Epidote (Ganghe, Dabie UHP Terrane). *Journal of Metamorphic Geology*, 31(4): 415–435. <https://doi.org/10.1111/jmg.12027>
- Guo, S., Ye, K., Yang, Y.H., et al., 2014. In Situ Sr Isotopic Analyses of Epidote: Tracing the Sources of Multi-Stage Fluids in Ultrahigh-Pressure Eclogite (Ganghe, Dabie Terrane). *Contributions to Mineralogy and Petrology*, 167(2): 975. <https://doi.org/10.1007/s00410-014-0975-9>
- Harmon, R.S., Hoefs, J., 1995. Oxygen Isotope Heterogeneity of the Mantle Deduced from Global ^{18}O Systematics of Basalts from Different Geotectonic Settings. *Contributions to Mineralogy and Petrology*, 120(1): 95–114. <https://doi.org/10.1007/bf00311010>
- Huang, J., Guo, S., Jin, Q.Z., et al., 2019. Iron and Magnesium

- Isotopic Compositions of Subduction-Zone Fluids and Implications for Arc Volcanism. *Geochimica et Cosmochimica Acta*. <https://doi.org/10.1016/j.gca.2019.06.020>
- Huang, J., Ke, S., Gao, Y.J., et al., 2015. Magnesium Isotopic Compositions of Altered Oceanic Basalts and Gabbros from IODP Site 1256 at the East Pacific Rise. *Lithos*, 231: 53–61. <https://doi.org/10.1016/j.lithos.2015.06.009>
- Inglis, E.C., Debret, B., Burton, K.W., et al., 2017. The Behavior of Iron and Zinc Stable Isotopes Accompanying the Subduction of Mafic Oceanic Crust: A Case Study from Western Alpine Ophiolites. *Geochemistry, Geophysics, Geosystems*, 18(7):2562–2579.
- Li, S.G., Yang, W., Ke, S., et al., 2017. Deep Carbon Cycles Constrained by a Large-Scale Mantle Mg Isotope Anomaly in Eastern China. *National Science Review*, 4(1): 111–120. <https://doi.org/10.1093/nsr/nww070>
- Li, Y.L., Zheng, Y.F., Fu, B., 2005. Mössbauer Spectroscopy of Omphacite and Garnet Pairs from Eclogites: Application to Geothermobarometry. *American Mineralogist*, 90(1):90–100. <https://doi.org/10.2138/am.2005.1400>
- Martin, L.A.J., Wood, B.J., Turner, S., et al., 2011. Experimental Measurements of Trace Element Partitioning between Lawsonite, Zoisite and Fluid and Their Implication for the Composition of Arc Magmas. *Journal of Petrology*, 52(6): 1049–1075. <https://doi.org/10.1093/ptrology/egr018>
- Nebel, O., Arculus, R.J., Sossi, P.A., et al., 2013. Iron Isotopic Evidence for Convective Resurfacing of Recycled Arc-Front Mantle beneath Back-Arc Basins. *Geophysical Research Letters*, 40(22): 5849–5853. <https://doi.org/10.1002/2013gl057976>
- Nebel, O., Sossi, P.A., Bénard, A., et al., 2015. Redox-Variability and Controls in Subduction Zones from an Iron-Isotope Perspective. *Earth and Planetary Science Letters*, 432: 142–151. <https://doi.org/10.1016/j.epsl.2015.09.036>
- Pogge von Strandmann, P.A.E., Elliott, T., Marschall, H.R., et al., 2011. Variations of Li and Mg Isotope Ratios in Bulk Chondrites and Mantle Xenoliths. *Geochimica et Cosmochimica Acta*, 75(18): 5247–5268. <https://doi.org/10.1016/j.gca.2011.06.026>
- Schmidt, M.W., Poli, S., 1998. Experimentally Based Water Budgets for Dehydrating Slabs and Consequences for Arc Magma Generation. *Earth and Planetary Science Letters*, 163(1–4): 361–379. [https://doi.org/10.1016/S0012-821X\(98\)00142-3](https://doi.org/10.1016/S0012-821X(98)00142-3)
- Scott, S.R., Sims, K.W.W., Frost, B.R., et al., 2017. On the Hydration of Olivine in Ultramafic Rocks: Implications from Fe Isotopes in Serpentinites. *Geochimica et Cosmochimica Acta*, 215:105–121. <https://doi.org/10.1016/j.gca.2017.07.011>
- Sossi, P.A., Nebel, O., Foden, J., 2016. Iron Isotope Systematics in Planetary Reservoirs. *Earth and Planetary Science Letters*, 452: 295–308. <https://doi.org/10.1016/j.epsl.2016.07.032>
- Teng, F.Z., Dauphas, N., Huang, S.C., et al., 2013. Iron Isotopic Systematics of Oceanic Basalts. *Geochimica et Cosmochimica Acta*, 107:12–26. <https://doi.org/10.1016/j.gca.2012.12.027>
- Teng, F.Z., Hu, Y., Chauvel, C., 2016. Magnesium Isotope Geochemistry in Arc Volcanism. *Proceedings of the National Academy of Sciences*, 113(26): 7082–7087. <https://doi.org/10.1073/pnas.1518456113>
- Teng, F.Z., Li, W.Y., Ke, S., et al., 2010. Magnesium Isotopic Composition of the Earth and Chondrites. *Geochimica et Cosmochimica Acta*, 74(14): 4150–4166. <https://doi.org/10.1016/j.gca.2010.04.019>
- Turner, S., Williams, H., Piazzolo, S., et al., 2018. Sub-Arc Xenolith Fe-Li-Pb Isotopes and Textures Tell Tales of Their Journey through the Mantle Wedge and Crust. *Geology*, 46(11): 947–950. <https://doi.org/10.1130/G45359.1>
- Wang, S.J., Teng, F.Z., Li, S.G., et al., 2014. Magnesium Isotopic Systematics of Mafic Rocks during Continental Subduction. *Geochimica et Cosmochimica Acta*, 143:34–48. <https://doi.org/10.1016/j.gca.2014.03.029>
- Wang, S.J., Teng, F.Z., Li, S.G., et al., 2017. Tracing Subduction Zone Fluid-Rock Interactions Using Trace Element and Mg-Sr-Nd Isotopes. *Lithos*, 290/291:94–103. <https://doi.org/10.1016/j.lithos.2017.08.004>
- Weyer, S., Ionov, D.A., 2007. Partial Melting and Melt Percolation in the Mantle: The Message from Fe Isotopes. *Earth and Planetary Science Letters*, 259(1–2): 119–133. <https://doi.org/10.1016/j.epsl.2007.04.033>
- Williams, H., Peslier, A., McCammon, C., et al., 2005. Systematic Iron Isotope Variations in Mantle Rocks and Minerals: The Effects of Partial Melting and Oxygen Fugacity. *Earth and Planetary Science Letters*, 235(1–2): 435–452. <https://doi.org/10.1016/j.epsl.2005.04.020>
- Zheng, Y.F., Fu, B., Gong, B., et al., 2003. Stable Isotope Geochemistry of Ultrahigh Pressure Metamorphic Rocks from the Dabie-Sulu Orogen in China: Implications for Geodynamics and Fluid Regime. *Earth-Science Reviews*, 62(1–2):105–161. [https://doi.org/10.1016/S0012-8252\(02\)00133-2](https://doi.org/10.1016/S0012-8252(02)00133-2)